

In situ activation of cobalt cathodes in alkaline water electrolysis

J. Y. HUOT, L. BROSSARD

Institut de recherche d'Hydro-Québec (IREQ), 1800 Montée Ste-Julie, Varennes, Québec, Canada J0L 2P0

Received 10 December 1987

The hydrogen evolution reaction (HER) on polished pure cobalt cathodes in 30 w/o KOH at 70°C in the presence of dissolved metallic impurities has been investigated in constant current and potential modes combined with the potential-sweep method. Potentiostatic tests show that the cell current decreases with time during the first 1000 s, which is tentatively attributed to the penetration of atomic hydrogen into the metal lattice. The deposition of copper, iron and zinc, observed after several hours' incubation significantly influences the Tafel parameters for HER.

Marked improvement in the electrocatalytic activity of the cathode in the presence of dissolved sodium molybdate is ascribed mainly to the deposition of molybdenum on the electrode surface, which lowers the Tafel slope and considerably increases the exchange-current density. The current increase is observed after an incubation period which is closely related to the concentration of dissolved sodium molybdate, whereas the rate of current increase with time is largely influenced by the applied potential.

1. Introduction

Recent studies of the hydrogen evolution reaction (HER) on polished pure nickel cathodes in 30 w/o KOH at 70°C have been carried out in the presence of KOH metallic impurities [1, 2] in a current-density range similar to or wider than those used in industrial electrolyzers. They showed that the penetration of atomic hydrogen into the metal lattice and the deposition of iron on the cathode surface are both detrimental to the hydrogen discharge. The same authors have reported that the addition of molybdate to the electrolyte significantly improves the electrocatalytic activity of the cathode [2].

The Tafel parameter values at 25°C and 6M KOH are approximately the same for polished cathodes of pure nickel or pure cobalt [3]. A valid comparison of the two metals at 70°C calls for determination of the Tafel parameters on a cobalt cathode and the anticipated time effects on its performance.

The present investigation focuses on the time effect on the HER on polished pure cobalt cathodes in 30 w/o KOH at 70°C in the presence of KOH metallic impurities at concentrations found in industrial electrolyzers. *In situ* activation of cobalt cathodes by adding sodium molybdate is also reported.

2. Experimental details

2.1. Cell and accessories

A conventional electrochemical cell of polysulphone was used with a cobalt working electrode, a nickel counterelectrode, and a Hg/HgO/KOH 1M reference electrode. The working electrode consisted of a vertical cobalt wire (Puratronic, 99.997%) with a diameter

of 0.05 cm, which gave a sample surface area of 0.19 cm². The samples were not exposed to heat treatment prior to the experiments. Triple-distilled water was used to prepare the solutions. The KOH pellets were certified A.C.S. (Fisher Scientific). A 5 cm² nickel counterelectrode (Mat. Res. Co., 99.99%) was surrounded by a polysulphone tube open at the bottom to minimize gaseous oxygen transfer from anolyte to catholyte during electrolysis.

The reference electrode was immersed in the upper section of the Luggin capillary tube (70°C), whose end was only ≈ 2 mm from the surface of the working electrode.

2.2. Test procedure

The sample was polished with 1 μ m alumina paste and rinsed with distilled water before being immersed in the solution which had undergone 1 h of nitrogen bubbling.

2.3. Experimental techniques

The temperature was held constant at 70°C throughout the experiments by means of a HAAKE D3 thermostatic bath. Polarization curves were obtained by standard techniques for a sweep rate of 1 mV s⁻¹ after the working-electrode potential had been held at a constant value for a given period of time using a PAR MODEL 273 potentiostat with an Apple II computer. The current was recorded against time at constant potential.

Since the current value was several mA cm⁻², the ohmic drop was significant with typical ohmic half-cell resistance values ranging from 0.05 to 0.1 Ω cm².

In an independent set of experiments, the reversible

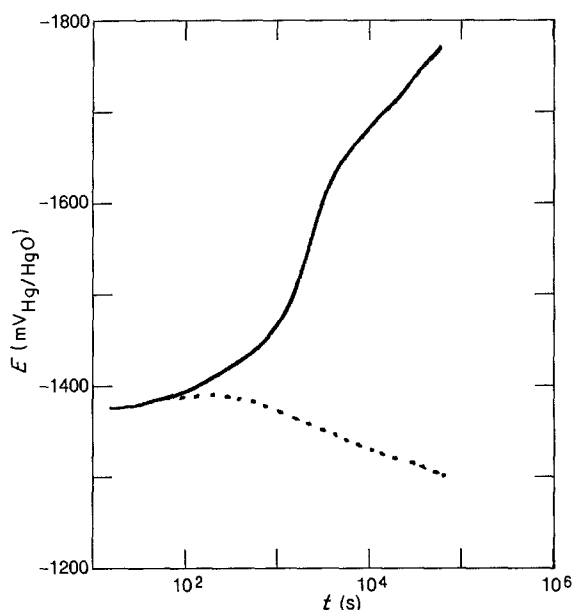


Fig. 1. Cobalt cathode potential behaviour plotted against time under galvanostatic control at 100 mA cm^{-2} in 30 w/o KOH (70°C) in the absence of dissolved $\text{Na}_2\text{MoO}_4 \cdot 2\text{H}_2\text{O}$ (full line) and in the presence of dissolved $\text{Na}_2\text{MoO}_4 \cdot 2\text{H}_2\text{O}$ (dashed line).

potential for the hydrogen reaction was measured by bubbling hydrogen against a platinized platinum electrode immersed in 30 w/o KOH solution at 70°C . The value was -0.952 V with respect to the Hg/HgO/KOH 1M reference electrode.

In addition, the cathode surface was examined by SEM and X-ray microanalysis (EDX) to determine its nature and morphology. The main metallic impurities in the solutions were aluminium (2.5 p.p.m.), lead (2.3 p.p.m.), chromium (1.3 p.p.m.), nickel (0.6 p.p.m.) and iron (0.5 p.p.m.) plus copper (< 0.1 p.p.m.).

All potential values for the electrodes are given with respect to the Hg/HgO/KOH 1M reference electrode at 70°C , unless otherwise mentioned.

3. Results

3.1. Galvanostatic experiments

Figure 1 shows a typical potential-time curve for an applied constant current of 100 mA cm^{-2} (full line). The potential is not corrected for the ohmic drop. The cathode half-cell potential can be seen to increase with time, the relationship between the potential and $\log t$ showing two linear regions. The value of $dE/d \log t$ is $117 \text{ mV decade}^{-1}$ time for times exceeding 5000 s. Similar behaviour is reported [1] for nickel cathodes under the same experimental conditions. The value of $dE/d \log t$ is $132 \text{ mV decade}^{-1}$ time from 60 000 to 200 000 s.

3.2. Potentiostatic experiments

The cathodes were held at a constant potential of $-1.5 \text{ V}_{\text{Hg/HgO}}$ immediately after immersion and the change in cell current was recorded. The I against $\log t$ curve in Fig. 2 shows that the current decreases up

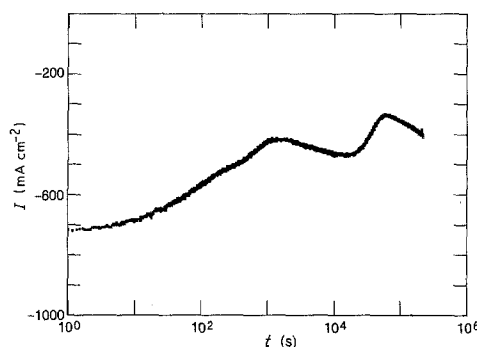


Fig. 2. Cobalt cathode current density behaviour plotted against time for potentiostatic control at $-1.5 \text{ V}_{\text{Hg/HgO}}$ in 30 w/o KOH at 70°C (in the absence of dissolved sodium molybdate).

to 1000 s, the relationship I against $\log t$ being linear from 30 to 1000 s with a slope of $270 \text{ mA cm}^{-2} \text{ decade}^{-1}$ time. A slow increase in current is noticed for $t \geq 1000$ s, I being equal to $\sim 440 \text{ mA cm}^{-2}$ at 1000 s compared to $\sim 460 \text{ mA cm}^{-2}$ at 16 000 s.

The hydrogen evolution parameters for cobalt cathodes were determined at various times with the applied electrode potential held constant at $-1.5 \text{ V}_{\text{Hg/HgO}}$. After a given time at this value, the potential was varied in the anodic direction at a constant sweep rate of 1 mV s^{-1} . Since the electrocatalytic activity at a given current density depends on the values of i_0 and b (summarized in Table 1), the hydrogen overpotential was calculated for a current of 250 mA cm^{-2} for each set of b and i_0 values from the well known relationship

$$\eta_{250} = b \log_{10} (i/i_0) \quad (1)$$

where η_{250} is the hydrogen overpotential corresponding to a current i of 250 mA cm^{-2} .

The calculated values of η_{250} at various times indicate that the electrocatalytic activity changes only slightly with time in contrast with the Tafel parameters. For example, the Tafel slope increases from $99 \text{ mV decade}^{-1}$ at 100 s to $182 \text{ mV decade}^{-1}$ at 2.4×10^5 s while the i_0 values increase from $0.18 \times 10^{-5} \text{ A cm}^{-2}$ at 100 s to $62 \times 10^{-5} \text{ A cm}^{-2}$ at 2.4×10^5 s. This significant variation of the Tafel parameters suggests that the reaction mechanism also changes considerably with time.

Table 1. Hydrogen evolution parameters for cobalt cathodes determined at various times during potentiostatic polarizations

Time at $-1.5 \text{ V}_{\text{Hg/HgO}}$ (s)	b (mV decade $^{-1}$)	i_0 (A cm 2)	η_{250} (mV)*
100	98.8	0.18×10^{-5}	508
1000	105	0.4×10^{-5}	503
2000	105	0.4×10^{-5}	506
10 000	108	0.65×10^{-5}	493
60 000	132	6.5×10^{-5}	473
120 000	191	83×10^{-5}	473
240 000	182	62×10^{-5}	475

* η_{250} is the calculated hydrogen overpotential for a current of 250 mA cm^{-2} .

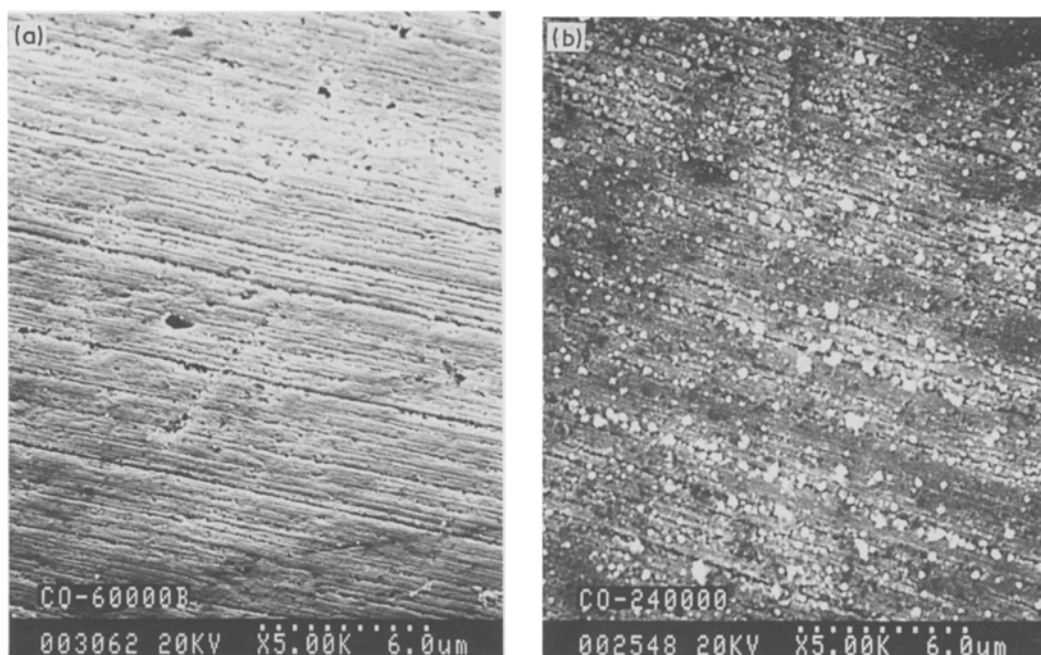


Fig. 3. Cathode surface during hydrogen discharge at $-1.5 V_{\text{Hg}/\text{HgO}}$ in 30 w/o KOH at 70°C . Removal times: (a) 60 000 s, (b) 240 000 s (in the absence of dissolved sodium molybdate). The current–time curve is given in Fig. 2.

3.3. Examination of the electrode surface

The morphology and nature of the cathode surface were investigated by SEM and X-ray microanalysis (EDX) to determine whether the metallic impurities present in the solution were deposited during electrolysis. The applied potential was constant at $-1.5 V_{\text{Hg}/\text{HgO}}$ and the corresponding current–time curve was that of Fig. 2.

The samples were examined after polarization times ranging from 0 to 240 000 s. For 0 s, the surface was smooth and only cobalt was detected (Table 2). Metallic impurities (copper, iron, zinc) began to be detected on the cathode surface after 60 000 s of polarization but from 60 000 to 240 000 s the amounts increased significantly. In addition, the presence of very small particles on the cobalt surface was noticed after 60 000 s of polarization (Fig. 3a). The size of these particles was larger at $t = 240 000$ s (Fig. 3b), from which it is deduced that they result from the deposition of metallic impurities on the cobalt substrate.

Table 2. Composition of the cathode surface by EDX analysis determined at various times at a constant potential of $-1.5 V_{\text{Hg}/\text{HgO}}$

Time (s)	Elements in atomic %			
	Co	Cu	Fe	Zn
0	100	0	0	0
100	100	0	0	0
1000	100	0	0	0
10 000	100	0	0	0
60 000	94	2	1.8	2.2
120 000	85	12	1.3	1.6
240 000	82	8	2.1	7.9

3.4. Recovery of lost efficiency

Molybdenum in the form of $\text{Na}_2\text{MoO}_4 \cdot 2\text{H}_2\text{O}$ was dissolved in the electrolyte prior to the immersion of the cobalt electrode. For an applied constant current of 100 mA cm^{-2} , it is observed that the cathode half-cell potential decreases with time in the presence of 4 mM sodium molybdate (dashed line of Fig. 1). In another set of experiments, a constant potential of $-1.5 V_{\text{Hg}/\text{HgO}}$ (not IR-corrected) was applied and the current was recorded against time for three molybdate concentrations: 0.1, 4 and 10 mM (Fig. 4). The presence of molybdenum causes an appreciable increase in current after an incubation period, τ , related to the concentration of dissolved molybdenum.

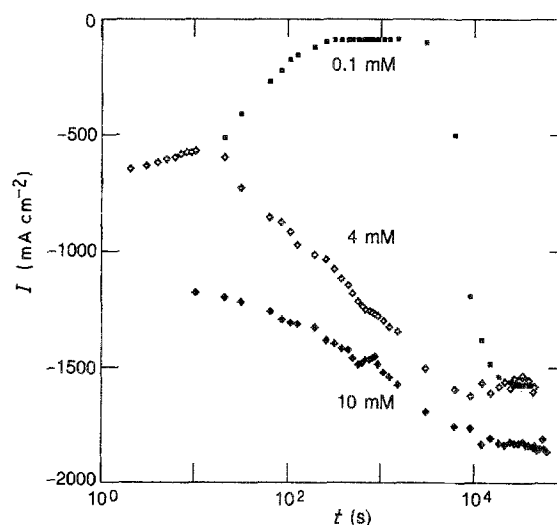


Fig. 4. Cobalt cathode current density plotted against time in the presence of molybdenum dissolved in the electrolyte. The constant applied potential is $-1.5 V_{\text{Hg}/\text{HgO}}$. Solution: 30 w/o KOH at 70°C with 0.1, 4 and 10 mM dissolved molybdate.

Table 3. Composition of the cathode surface by EDX analysis determined at various times in the presence of 4 mM dissolved sodium molybdate ($-1.5 V_{\text{Hg/HgO}}$)

Time (s)	Elements in atomic %				
	Co	Cu	Fe	Mo	Zn
100	99.3	0.5	0	0.2	0
10 000	83.7	2.8	2.3	11.2	0
60 000	70.4	4.3	5.0	20.3	traces
240 000	11.3	10.4	21	57.3	traces

For example, after 3000 s of deactivation the current density increased from 90 to 1600 mA cm⁻² at 20 000 s in the presence of 0.1 mM dissolved molybdenum. In addition, τ , is markedly shorter when the molyb-

denum concentration is increased: it is as little as ~ 150 s for 4 mM and just a few seconds for 10 mM.

EDX analysis of the cathode at various times in the presence of 4 mM dissolved sodium molybdate at $-1.5 V_{\text{Hg/HgO}}$ (Table 3) indicates that the copper iron and molybdenum contents increase substantially with polarization times from 100 to 240 000 s and become considerable when the polarization time exceeds τ . SEM examination of the cathode surface (Fig. 5) reveals the formation of a deposit for $t > \tau$, the morphology of the deposit being different after 10 000 s (Fig. 5b), 60 000 s (Fig. 5c) and 240 000 s (Fig. 5d) of polarization. The surface roughness tends to increase from 10 000 to 60 000 s while the deposit becomes relatively porous over 60 000 s.

The anodic portions of single-cycle voltammograms

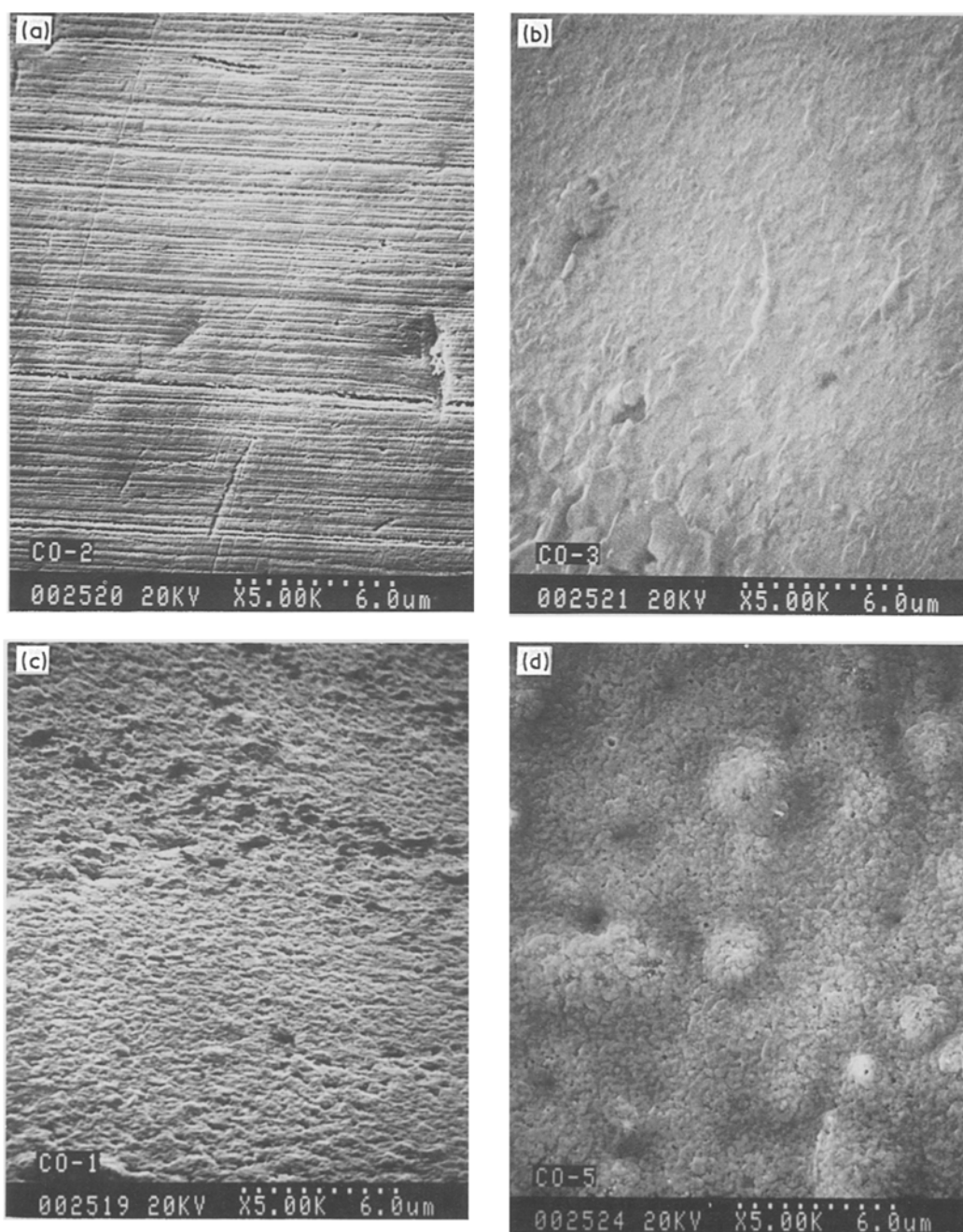


Fig. 5. Cathode surface during hydrogen discharge at $-1.5 V_{\text{Hg/HgO}}$ in the presence of 4 mM sodium molybdate (30 w/o KOH, 70°C). Removal times are (a) 100 s, (b) 10 000 s, (c) 60 000 s, (d) 240 000 s. The current-time curve is given in Fig. 4.

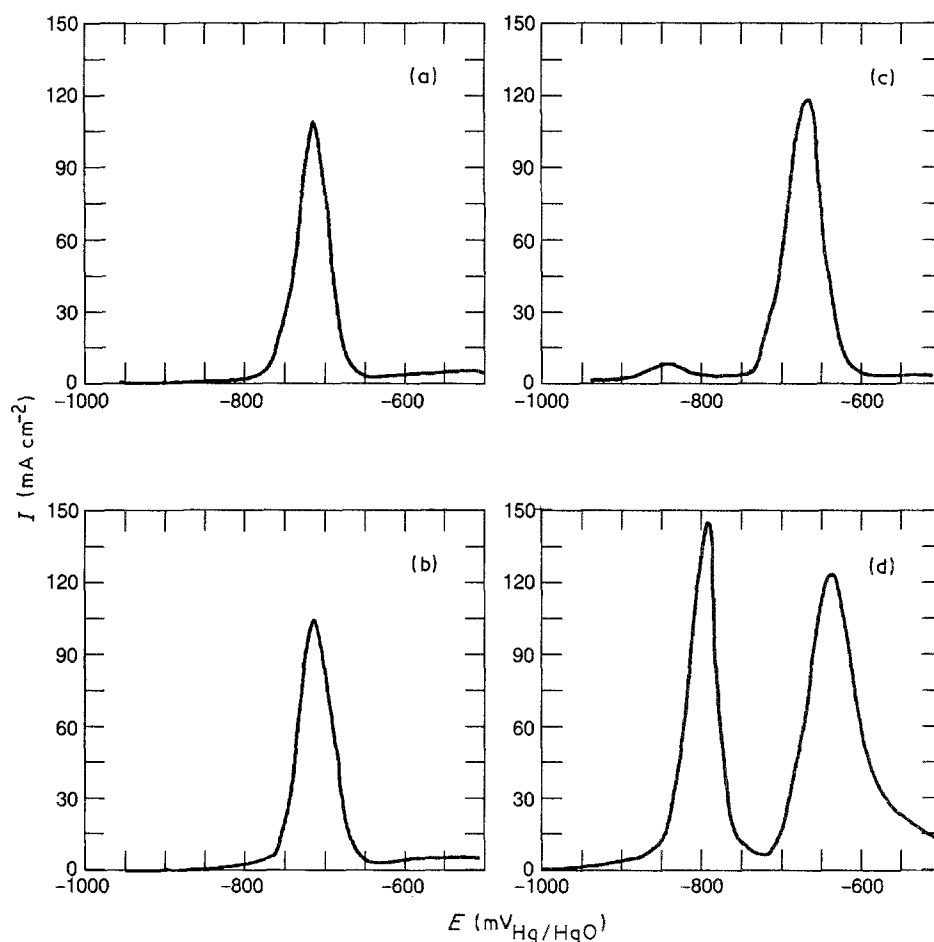


Fig. 6. Influence of the cathode polarization time at $-1.5 V_{\text{Hg/HgO}}$ on the anodic portion of the single-cycle voltammograms in the presence of $4 \text{ mM Na}_2\text{MoO}_4$ (30 w/o KOH at 70°C). The initial applied potential was $-1.5 V_{\text{Hg/HgO}}$ for (a) 100 s, (b) 1000 s, (c) 10 000 s, (d) 60 000 s.

for cobalt cathodes are illustrated in Fig. 6. A constant potential of $-1.5 V_{\text{Hg/HgO}}$ was applied during a time ranging from 100 to 240 000 s in the presence of $4 \text{ mM Na}_2\text{MoO}_4 \cdot 2\text{H}_2\text{O}$. The electrodes were then potenti-

dynamically swept from -1.5 to $+0.7 V_{\text{Hg/HgO}}$ at a scan rate of 10 mVs^{-1} . A strong dependence of the shape of the voltammogram on the polarization time at $-1.5 V_{\text{Hg/HgO}}$ is observed. A second oxidation

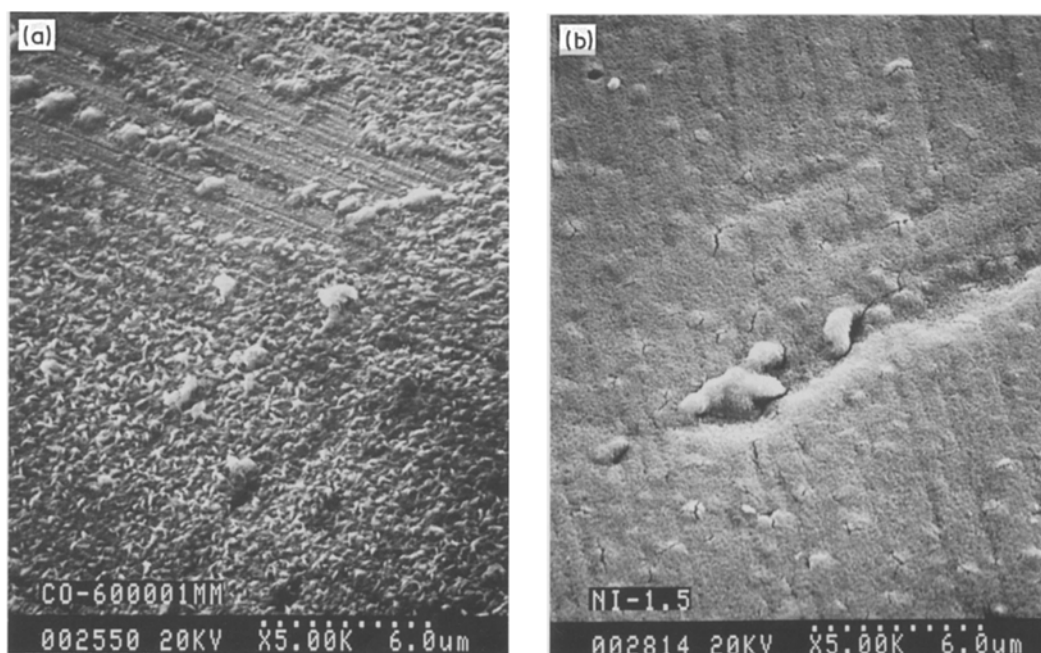


Fig. 7. Influence of sodium molybdate concentration on cathode surface during hydrogen discharge at $-1.5 V_{\text{Hg/HgO}}$ (30 w/o KOH, 70°C). Removal time: 60 000 s. Sodium molybdate concentration: (a) 0.1 mM , (b) 10 mM . EDX analysis of the surface: (a) copper 89.8 at. %, Cu 8.9 at. %, Fe 0 at. %, Mo 1.3 at. %, Zn traces, (b) Co 81.3 at. %, Cu 6.4 at. %, Fe 1.7 at. %, Mo 10.6 at. %, Zn traces. The current-time curves are given in Fig. 4.

wave is present as soon as the concentration of impurities on the electrode surface becomes appreciable (Table 3), i.e. for $t \approx 10\,000$ s. The first anodic peak (peak I) has a maximum at $-0.84 V_{\text{Hg}/\text{HgO}}$ (E_1) compared to $-0.67 V_{\text{Hg}/\text{HgO}}$ (E_{II}) for peak II; the charge corresponding to peak I (Q_1) is only 0.045 C cm^{-2} compared to $\sim 0.7 \text{ C cm}^{-2}$ for peak II (Q_{II}) at $t = 10\,000$ s. From $10\,000$ to $240\,000$ s of polarization, Q_{II} , E_1 and E_{II} are practically constant with time whereas Q_1 is 0.69 C cm^{-2} at $t = 60\,000$ s compared to 1.38 C cm^{-2} at $t = 240\,000$ s. It is concluded that peak I corresponds to the electrochemical oxidation of molybdenum [2].

To investigate the nature of peak II, the anodic portions of single-cycle voltammograms for cobalt cathodes were determined under the same experimental conditions as those of Fig. 6, except that the solution was free of molybdate. The constant potential was applied for a time ranging from 100 to $240\,000$ s. For t less than or equal to $10\,000$ s, the cobalt surface is bare (Table 2) and only one oxidation peak is observed at $\sim -0.67 V_{\text{Hg}/\text{HgO}}$, which corresponds to the oxidation of cobalt, its charge being $\sim 0.74 \text{ C cm}^{-2}$. For $60\,000$ s, an additional peak associated with the oxidation of deposited iron is also present, reaching a maximum at $\sim -0.5 V_{\text{Hg}/\text{HgO}}$, as previously reported for iron deposits on nickel substrates [2]. Its charge is $\sim 0.1 \text{ C cm}^{-2}$. For $t > 60\,000$ s, the peaks cannot be separated while their maximum is at $\sim -0.67 V_{\text{Hg}/\text{HgO}}$, and their charge is $\sim 1.1 \text{ C cm}^{-2}$ at $240\,000$ s. On this basis, it is tentatively concluded that peak II in Fig. 6, i.e. in the presence of dissolved molybdenum, is due to the oxidation of cobalt and possibly of iron when present on the surface.

The morphology and composition of the deposit and the Tafel parameters associated with the hydrogen evolution are also dependent on the concentration of the dissolved sodium molybdate. Figure 7 shows the cathode surface for a removal time of $60\,000$ s after polarization under the experimental conditions of Fig. 4, with 0.1 or 10 mM of dissolved Na_2MoO_4 . The current can be considered practically constant with time at $\sim 60\,000$ s (Fig. 4) in this range of sodium molybdate concentration. The surface roughness of the cathode is intensified by the presence of a deposit between 0.1 and 4 mM dissolved sodium molybdate (Figs 7a and 5c respectively). For 10 mM (Fig. 7b), the general morphology of the film suggests that the deposit is rather porous and the presence of small cracks is also observed. The surface concentrations of iron and molybdenum are at their maximum for 4 mM in $\text{Na}_2\text{MoO}_4 \cdot 2\text{H}_2\text{O}$. The charge corresponding to the oxidation peak of molybdenum indicates that a larger amount of molybdenum is deposited on the electrode surfaces from 4 mM dissolved molybdate than from 10 mM , the ratio being ~ 35 . The corresponding values of the hydrogen evolution parameters i_0 and b for those electrodes are $51.4 \times 10^{-5} \text{ A cm}^{-2}$ and 106 mV for 0.1 mM in $\text{Na}_2\text{MoO}_4 \cdot 2\text{H}_2\text{O}$, $126 \times 10^{-5} \text{ A cm}^{-2}$ and 114 mV

Table 4. Hydrogen evolution parameters determined at various times in the presence of 4 mM sodium molybdate

Time at $-1.5 V_{\text{Hg}/\text{HgO}}$ (s)	b (mV decade $^{-1}$)	i_0 (A cm^{-2})	η_{250} (mV)
100	86.2	0.39×10^{-5}	414
1000	87.5	3.1×10^{-5}	342
10 000	71.5	2.5×10^{-5}	286
60 000	114	126×10^{-5}	262
240 000	169	1642×10^{-5}	200

for 4 mM (Table 4) and $104 \times 10^{-5} \text{ A cm}^{-2}$ and 120 mV for 10 mM .

Figure 8 shows the current against time at three different values of constant applied potential: -1.3 , -1.4 and $-1.5 V_{\text{Hg}/\text{HgO}}$ in the presence of 4 mM dissolved sodium molybdate. A higher applied potential results in a higher current for all times. The values of the slope $dI/d \log t$ in the region for which the I against $\log t$ relationship is linear are $433 \text{ mA cm}^{-2} \text{ decade}^{-1}$ time at $-1.5 V_{\text{Hg}/\text{HgO}}$, $384 \text{ mA cm}^{-2} \text{ decade}^{-1}$ time at $-1.4 V_{\text{Hg}/\text{HgO}}$ and $260 \text{ mA cm}^{-2} \text{ decade}^{-1}$ time at $-1.3 V_{\text{Hg}/\text{HgO}}$. For polarization times exceeding $\sim 20\,000$ s, the current may be considered relatively constant with time. The charge corresponding to the oxidation of molybdenum (Q_1) after $60\,000$ s of polarization is 0.69 , 0.06 and $\sim 0 \text{ C cm}^{-2}$ at potentials of -1.5 , -1.4 and $-1.3 V_{\text{Hg}/\text{HgO}}$, respectively.

The hydrogen evolution parameters for cobalt cathodes determined at various times during potentiostatic polarization at $-1.5 V_{\text{Hg}/\text{HgO}}$ in the presence of 4 mM sodium molybdate are summarized in Table 4. The same procedure was used for determining the i_0 and b values for Tables 1 and 4. It is observed that η_{250} decreases significantly from 414 mV at 100 s of polarization time to 200 mV at $240\,000$ s of polarization time.

The values of η_{250} for nickel and cobalt substrates are plotted against time in Fig. 9. Those for cobalt were calculated from the Tafel parameters, which were being determined after maintaining the electrode potential at $-1.5 V_{\text{Hg}/\text{HgO}}$ for a time t in the presence of 4 mM dissolved Na_2MoO_4 . Under these conditions, it

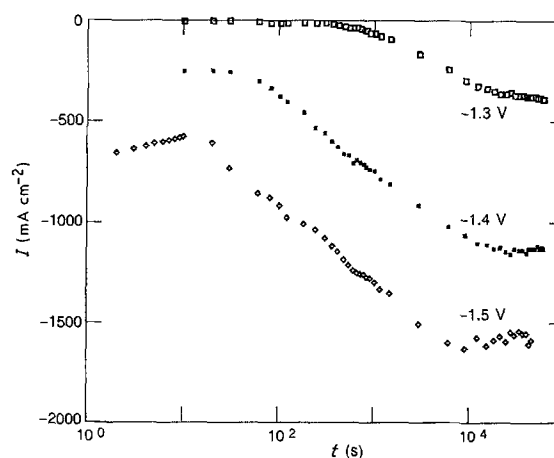


Fig. 8. Cobalt cathode current density behaviour plotted against time for potentiostatic control at $-1.5 V_{\text{Hg}/\text{HgO}}$, $-1.4 V_{\text{Hg}/\text{HgO}}$ and $-1.3 V_{\text{Hg}/\text{HgO}}$ in the presence of 4 mM dissolved sodium molybdate (30 w/o KOH , 70° C).

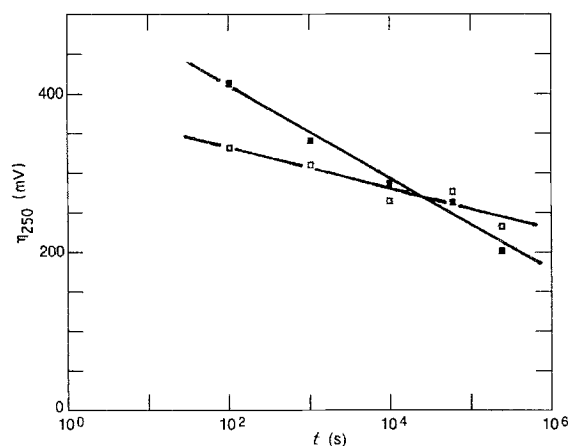


Fig. 9. The values of η_{250} plotted against time for nickel (\square) and cobalt (\blacksquare) substrates in the presence of 4 mM dissolved Na_2MoO_4 . The values of η_{250} for nickel are given in the literature [2] and for cobalt in Table 4.

is observed that *in situ* activation is stronger on a cobalt than on a nickel substrate and that the hydrogen overpotential tends to be practically the same for both substrates after $\sim 100\,000$ s of polarization.

4. Discussion

The typical current–time curve at a given applied electrode potential of $-1.5 V_{\text{Hg}/\text{HgO}}$ in Fig. 2 is arbitrarily divided into two distinct regions. From ~ 100 to $\sim 10\,000$ s (region a), the surface of the cobalt cathode is free of impurities (Table 2) and the Tafel parameters are relatively constant (Table 1). For longer times (region b), the accumulation of impurities on the cobalt surface (Table 2) results in significant changes both in its morphology (Fig. 3) and in the Tafel parameters (Table 1).

As long as the cobalt surface is bare, current decay is most probably related to the absorption of atomic hydrogen into the metal lattice, as suggested for a parent metal, nickel [1]. According to Amossé and Barbier [4], this creates a potential difference between the metal, i.e. in the first layer, and the solution, which tends to oppose current flow. On the other hand, the absence of an anodic peak before the oxidation of cobalt is noticed as the potential is swept at 10 mV s^{-1} after cathodic polarization at -1.3 , -1.4 and $-1.5 V$ for 1000 s. It is tentatively deduced that hydrogen dissolved in the bulk electrode is less accessible for cobalt than for nickel [1].

In the present investigation, the value of the slope $dI/d \log t$ at $-1.5 V_{\text{Hg}/\text{HgO}}$ in region a, is $270\text{ mA cm}^{-2}\text{ decade}^{-1}$ time for cobalt compared with $300\text{ mA cm}^{-2}\text{ decade}^{-1}$ time for nickel under the same experimental conditions [1]. The hydrogen penetration rate may depend on the nature of the electrode surface [5]. Furthermore, the rate-determining step for the hydrogen discharge is generally related to the morphology and nature of the electrode material [6]. For both reasons, it is anticipated that the Tafel parameters in the region for which the cathode surface is pure cobalt will be different from those observed in the region characterized by impurities. In fact, an increase in the

Tafel parameters (Table 1) becomes significant as soon as the accumulation of impurities is observed (Table 2).

The markedly improved electrocatalytic activity for the HER in the presence of dissolved sodium molybdate (Fig. 4) is ascribed mainly to the deposition of metallic molybdenum on the electrode surface (Table 3 and Fig. 5). This not only lowers the Tafel slope but considerably increases the exchange current density (Tables 1 and 4).

The significant increase in the exchange-current density from 10 000 to 240 000 s of polarization in the presence of 4 mM Na_2MoO_4 (Table 4) is consistent with the fact that both the surface roughness and the amount of deposited molybdenum tend to increase with time (Figs 5b, c, d). In addition, the surface deposition of zinc is almost completely impeded by the presence of molybdenum in the solution (Tables 2 and 3, Fig. 6).

With regard to the influence of sodium molybdate concentration for times longer than the incubation periods, minor changes noticed in the surface morphology from 0.1 to 10 mM (Figs 5c and 7) are in good agreement with the fact that the Tafel parameters for HER are practically the same for all surfaces.

The amount of molybdenum deposited (Q_1) is considerably larger after 60 000 s of polarization in the presence of 4 mM Na_2MoO_4 as the applied potential is raised from $-1.3 V_{\text{Hg}/\text{HgO}}$ to $-1.5 V_{\text{Hg}/\text{HgO}}$: it is approximately ten times higher at $-1.5 V_{\text{Hg}/\text{HgO}}$ than it is at $-1.4 V_{\text{Hg}/\text{HgO}}$, for example. Consequently, it is deduced that the molybdenum deposition rate is largely dependent on the applied potential value. The variation in the slope $dI/d \log t$ with the applied potential (Fig. 8) is believed to be due to the differences in the molybdenum deposition rate. The time-dependence of the electrocatalytic activity suggests that the final surface condition corresponds to an active metallic form of molybdenum arising from the direct reduction of deposited oxides by the adsorbed hydrogen during the intense hydrogen discharge [7]. The overpotential dependence of $dI/d \log t$ is explained by the increased hydrogen activity on the surface (i.e. the hydrogen coverage) at higher hydrogen overpotentials [8]. Consequently, the kinetics of the direct reduction of molybdenum oxide(s) by atomic hydrogen could be accelerated at more negative values of the applied potential.

Comparison of η_{250} values for nickel and cobalt substrates shows that nickel is a better electrocatalyst than cobalt in the region for which the substrate is bare, i.e. at shorter times (Fig. 9). The nature of the surface changes with time owing to the accumulation of molybdenum on both metals. The presence of molybdenum eventually dominates for long times and the overpotential for the HER becomes quite similar for cobalt and nickel cathodes.

5. Conclusion

The loss of efficiency of the hydrogen discharge on

cobalt cathodes takes the form of an increase in the cathodic overpotential at constant current density or a decrease in the cell current during the first 1000 s at constant cathode half-cell potential. The current decay with time is tentatively ascribed to the penetration of atomic hydrogen into the metal lattice by some diffusion process. Impurity deposits on the cathode surface are observed after several hours of incubation, which significantly influences the Tafel parameters.

The notable improvement in the electrocatalytic activity of the cathode observed at a given time in the presence of sodium molybdate in the electrolyte is attributed to the deposition of molybdenum on the surface which lowers the Tafel slope as well as considerably increasing the exchange-current density. Improvement of the hydrogen discharge is noticed

after an incubation period closely related to the concentration of sodium molybdate.

References

- [1] J. Y. Huot and L. Brossard, *Int. J. Hydrogen Energy* **12** (1987) 821.
- [2] J. Y. Huot and L. Brossard, *Surface and Coating Technology* **34** (1988) 373.
- [3] P. W. T. Lu and S. Srinivasan, *J. Electrochem. Soc.* **125** (1978) 265.
- [4] J. Amossé and M. J. Barbier, *Electrochim. Acta* **11** (1966) 1045.
- [5] H. Atrens, D. Mezzanotte, N. F. Fiore and M. A. Genshow, *Corrosion Sci.* **20** (1980) 673.
- [6] E. Yeager and D. Tryk, in Proceedings of the Symposium on "The Chemistry and Physics of Electrocatalysis," (edited by J. McIntyre, M. Weaver and E. Yeager) *Phys. Electrochem. Proc.*, **84** (1984) 827.
- [7] C. M. Lacnjevac and M. M. Jaksic, *J. Res. Inst. Catalysis, Hokkaido Univ.* **31** (1983) 7.
- [8] M. Enyo and T. Maoka, *J. Electroanal. Chem.* **108** (1980) 277.